Proceedings of the 7th International Conference on Mechanics and Materials in Design
Albufeira/Portugal 11-15 June 2017. Editors J.F. Silva Gomes and S.A. Meguid.
Publ. INEGI/FEUP (2017)

PAPER REF: 6986

ADVANCED MATERIAL DEVELOPMENT AND DESIGN OPTIMIZATION FOR IMPROVED PROPERTIES IN ADDITIVE MANUFACTURING PROCESS

Lukasz Matysiak[1(*)], Michal Kozupa[1], Bogdan Dybala[2]

[1]ABB Corporate Research, Krakow, Poland
[2]Department of Mechanical Engineering, Wroclaw University of Technology, Wroclaw, Poland
[(*)]*Email:* lukasz.matysiak@pl.abb.com

ABSTRACT

This work presents study on advanced materials development for 3D printing technology and describes the application of additive manufacturing process in producing structures with improved characteristics. The manufacturing method of functional materials is provided together with the results of computer simulations and laboratory tests performed to optimize and evaluate mechanical and electrical properties of the structures. This research allowed to work out the methodology for producing functional materials and to identify potential improvements of compression and dielectric strength that are possible by combining advanced materials, 3D printing technology and computer simulations.

Keywords: 3D printing, composites, geometry, optimization, mechanical, electrical.

INTRODUCTION

The aim of this study was to develop polymer based materials with enhanced functionality and additional benefits that can come with 3D printing technology, using computer simulations. After computer optimization mechanical and electrical parameters were determined experimentally and crucial characteristics of 3D printed samples have been defined.

In the first step mixture of ABS thermoplastic granules and carbon fibres (CF) were used in extrusion process to produce composite filaments with improved electrical conductivity. Different lengths of carbon fibres, filler levels, process operations and parameters were investigated to find the optimum material composition and processing.

The second part of research was focused on electrical and mechanical performance optimization of the 3D printed structures. For this purpose dielectric and mechanical computer simulations were performed for initial evaluation and for comparison of different design concepts. Next, some of designs were fabricated in 3D printing process and tested in laboratory environment to evaluate the compression strength and dielectric strength of the worked out geometrical concepts.

MATERIALS DEVELOPMENT

According to the performed literature search there were attempts in the field of composites development for additive manufacturing technology (Zhong, 2001; Moulart, 2004; Ning, 2015). In this research the first stage aimed at developing composite material in the form of

thermoplastic filament filled with carbon fibres that would be applicable to 3D printing Fused Filament Fabrication process. The goal was to obtain material having different electrical conductivity provided by the said carbon fibres. ABS thermoplastic was chosen as the composite matrix. Properties of typical ABS material are gathered in Table 1 (ABS Filament MSDS).

Table 1 - Properties of ABS

Physical state	Solid
Odour	None
pH	Not applicable
Density	1.03 g/cm3
Decomposition temperature	250°C
Autoignition temperature	466°C
Melting point/range	Softening above 100°C
Water solubility	Insoluble

Three different sizes of fibres were tested in terms of composite system development. Carbon fibres with the average length of about 4 mm (Fig. 1b) were clogging the extruder worm gear, so it was impossible to extrude this material. Eventually, because of technological capabilities (the nozzle of 3D printer having a diameter of 400 μm) the shortest and finely grounded fibres (Fig. 1a) were used. Fibres diameter was greater than 7 μm and their average length was 150-200 μm. The maximum length of a single carbon fibre was in the range 1000-1250 μm (Fig. 1). The basic properties of carbon fibres are presented in Table 2 (Carbon Fibre MSDS).

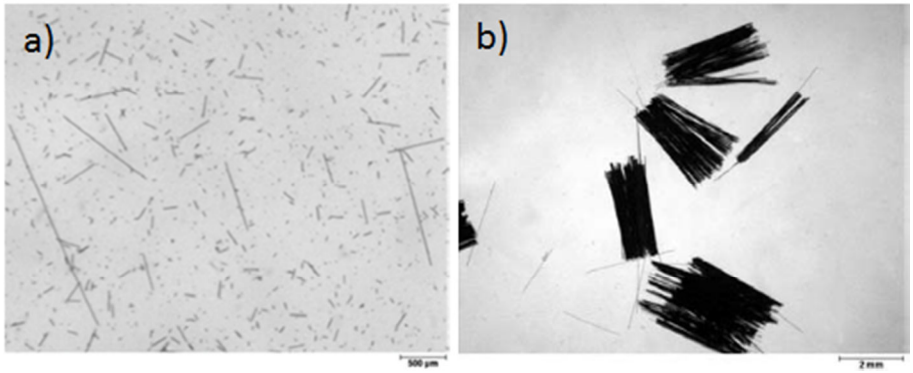

Fig. 1 - Carbon fibre with the average length: a) 150-200 μm, b) 4 mm [2]

Table 2 - Properties of fibres

Fibre type	Carbon
Colour	Grey/black
Odour	None
Specific gravity	1.78 g/cm3
Additional information	Electrically conductive

Different carbon fibres concentrations were investigated when developing the composite material. More precisely, ABS matrix was filled with 6 wt%, 12 wt% and 18 wt% of carbon fibres. After initial trials with the ABS+CF composite extrusion microscopic evaluation of the obtained structures was performed. It revealed problem with air voids formation inside the

composite structure and with fibres clustering making the properties of the composite material non-uniform. In this connection additional steps were introduced into the material formulation process including drying, granulation, rolling and milling. In total three different material formulation procedures were developed and tested as illustrated in Fig. 2.

ABS with 6 wt% CF was produced using two different procedures. In both cases the granules were dried, extruded, granulated, dried again, extruded again and granulated again. Next, in the A process the filament was subjected to rolling mill operation in a crusher roller and the resulting sheets of material were ground in a mill to yield composite flakes (refer to Fig. 3) which were then dried and extruded for the third time. In contrast in the B process the filament was only dried and granulated for the third time. Additional steps taken in the A process were designed to unify the composite by eliminating air bubbles and clusters of carbon fibres. The effect of improvements in ABS+CF composite formulation process can be observed in Fig. 4. Filaments 12 wt% and 18 wt% were produced according to the A procedure.

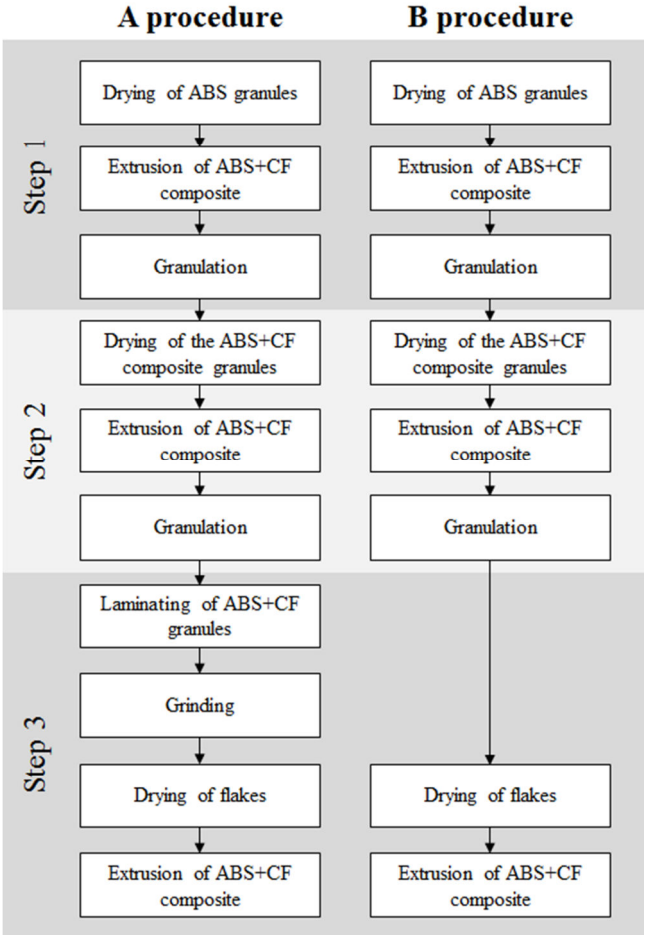

Fig. 2 - Different material formulation procedures developed and tested

COMPUTER SIMULATIONS

Development of material with properties given for the given application is only one side of the problem. Equally important aspect influencing the final quality and functionality of 3D printed part is its geometrical design. For this purpose design optimization study was

performed and it concerned two aspects, namely compression strength and dielectric performance of the evaluated structures. Investigations were based on computer simulations allowing one to analyse and optimize the mentioned properties of 3D printed geometries.

Fig. 3 - Material flakes after milling operation

The first part of numerical study were 3D mechanical analyses of 100x100x2 mm plates having different internal structures with compressive load acting on them from the top as presented in Fig. 5. The bottom walls of the said structures were mechanically constrained. It can be seen that main difference between the analysed geometries was the wall thickness. Honeycomb 1 structure had the thinnest walls, Honeycomb 3 had the thickest walls and walls in Honeycomb 2 structure was in the middle.

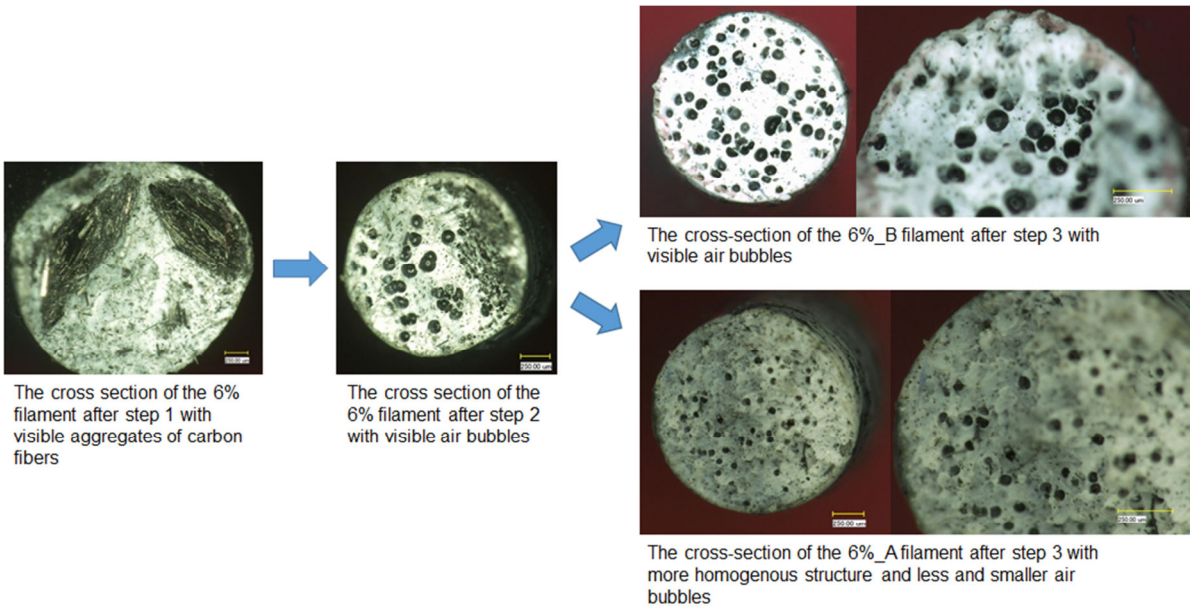

Fig. 4 - Effect of improvements in ABS+CF composite formulation process

The results of mechanical simulations are presented in Fig. 6 and Fig. 7. Fig. 6 depicts forces obtained for different analysed structures at 1% strain. It can be concluded that the solid geometry turned out to be superior to all honeycomb structures. The force value for the solid sample was around 300 kN, while for the honeycomb geometries it varied between 38 kN and 155 kN. Fig. 7 shows distribution of mechanical stresses in two selected honeycomb

structures. It can be concluded based on these results that thickening of the honeycomb structure decreased the values of stresses, what means also higher compression strength.

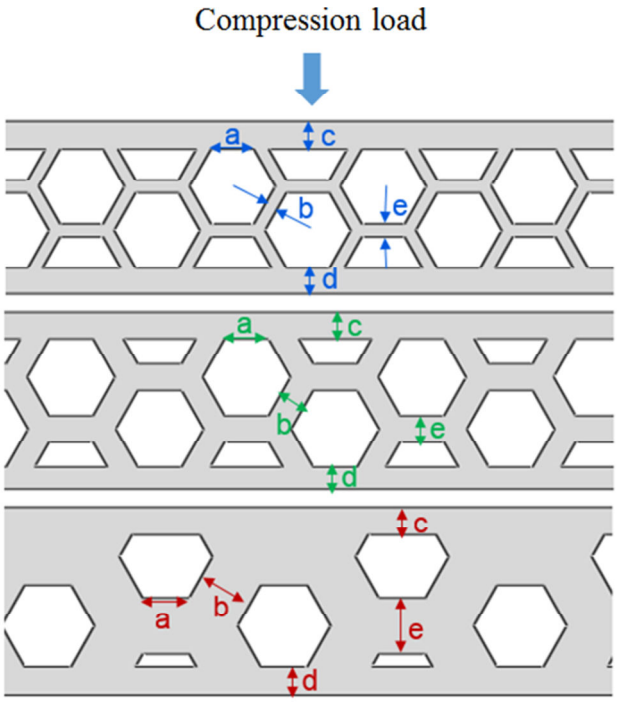

Structure	a	b	c	d	e
Honeycomb 1	0,5	0,15	0,3	0,251	0,15
Honeycomb 2	0,5	0,283	0,326	0,3	0,3
Honeycomb 3	0,5	0,6	0,3	0,3	0,6

Fig. 5 - Geometries considered in mechanical simulations

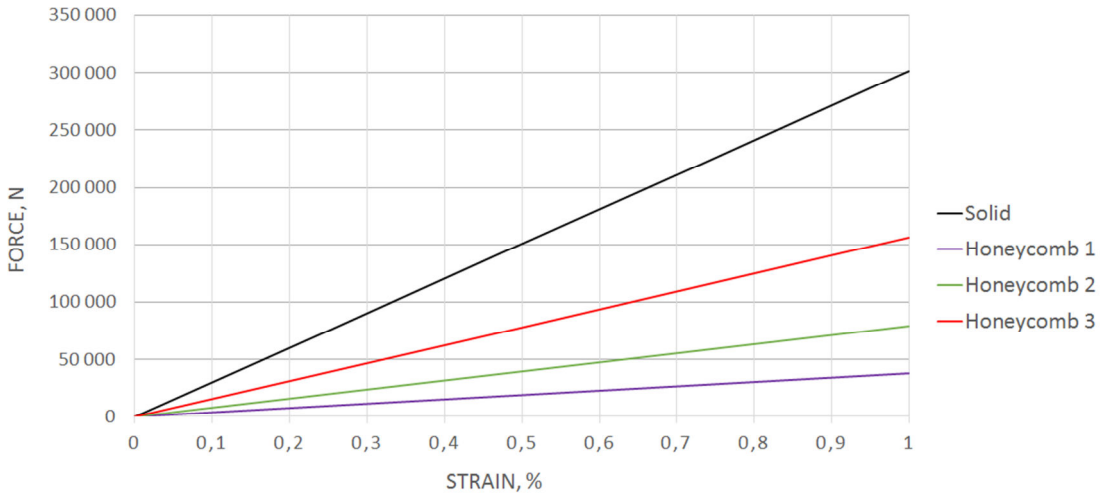

Fig. 6 - Results of mechanical simulations

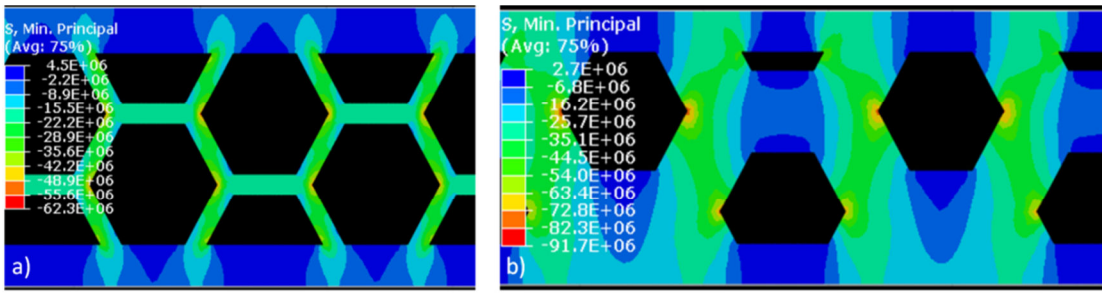

Fig. 7 - Distribution of mechanical stresses in the analysed structures: a) Honeycomb 1, b) Honeycomb 3

In the second part of numerical study different geometrical designs expressed by 2D model were investigated considering their dielectric performance. The configuration of the analysed system is presented in Fig. 8. It consisted of circular metal electrode on a potential of 1V, of grounded metal wall and thermoplastic barrier placed between them. All elements of the tested system were surrounded by insulating oil. Electrical permittivity of the oil and barrier material was defined on the level of 2.2 and 2.8 respectively. The barrier between the electrodes was either solid wall or had layered structure. Several different layered structures were investigated and they differed by the number of layers, layers thicknesses and distances between layers as shown in Fig. 9.

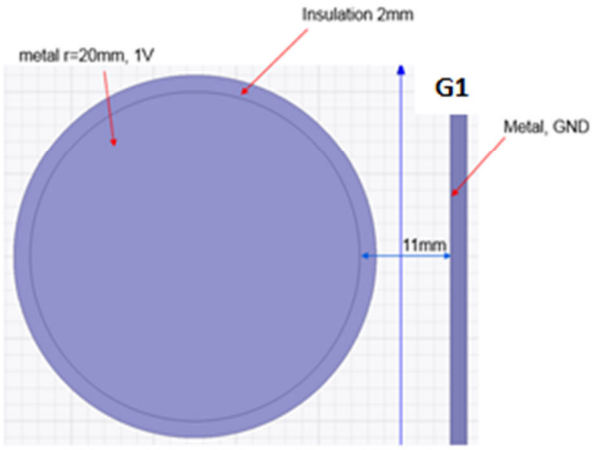

Fig. 8 - Configuration of the system with G1 barrier analysed in electrical simulations

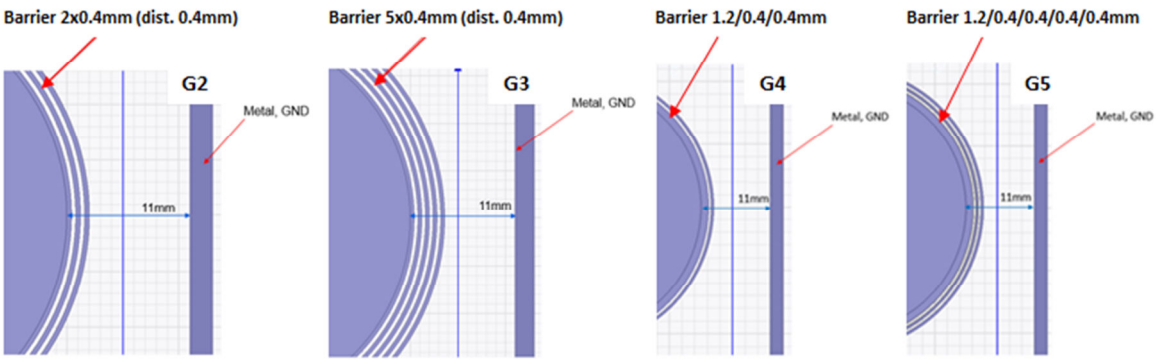

Fig. 9 - Different layered structures analysed in electrical simulations

The results of electrical simulations are presented in Fig. 10 and in Table 3. It can be concluded based on Fig. 10 that the electric field distribution is influenced by the barrier structure. It can also be stated analysing the values of maximum electric field gathered in Table 3 that the introduction of layered barriers can reduce the field strength in the barrier material at the cost of higher electric field in the oil between the barrier layers. Simultaneously, electric field in oil outside the barrier (between the barrier and the grounded wall) is reduced thanks to the layered structure of the barrier when compared to the reference solid barrier geometry (G1). In other words the mostly stressed oil volume is enclosed between the barrier layers what may reduce the probability of discharge inception. However, this observation has to be confirmed in real electrical tests.

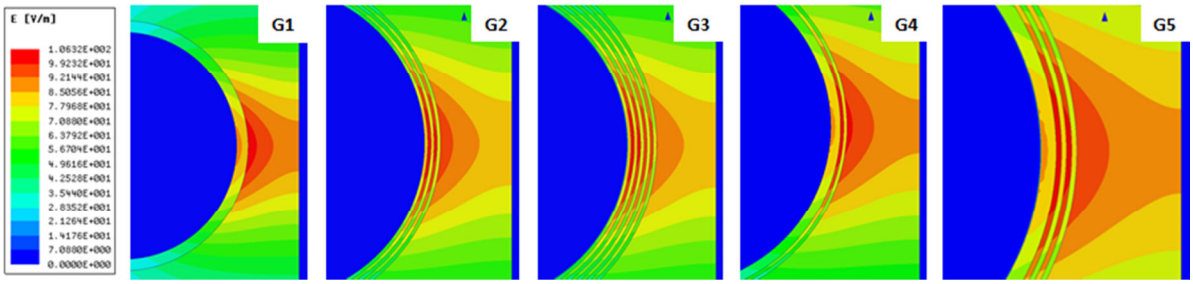

Fig. 10 - Distribution of electric field strength depending on the barrier structure

Table 3 - Maximum electric field observed in computer simulations

Geometry	G1	G2	G3	G4	G5
E_{max} in barrier material [V/m]	97.54	94.78	96.33	96.51	97.33
E_{max} in oil inside barrier [V/m]	103.96	109.16	110.93	106.31	107.26
E_{max} in oil outside barrier [V/m]	-	102.13	98.33	102.99	101.00

MECHANICAL TESTING

The performed numerical study was followed by experimental verification of different geometrical concepts including lattice-like and honeycomb-like structures that were compared with the reference solid counterpart. Samples had the shape of a right rectangular prism with dimensions: 10 x 10 x 4 mm as presented in Fig. 11 and Fig. 12.

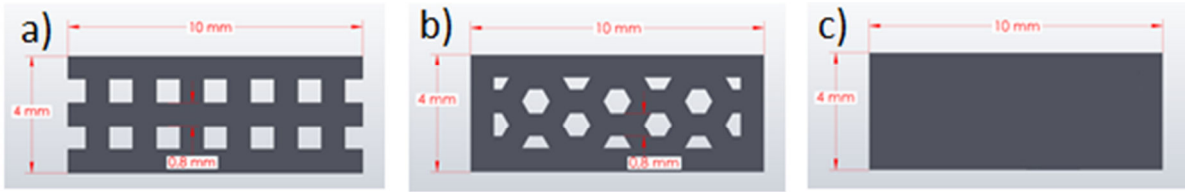

Fig. 11 - Geometrical concepts verified in mechanical tests: a) lattice, b) honeycomb, c) solid

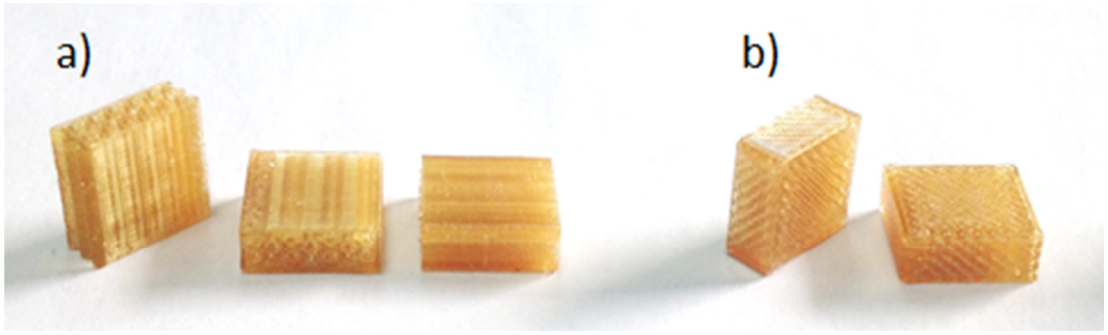

Fig. 12 - Specimens made of Ultem 1010 before testing: a) honeycomb structure, b) solid structure

In the first part of experimental study compressive properties of 3D printed thermoplastic structures were determined. Specimens were manufactured on Stratasys Fortus 450mc 3D printer in material extrusion process known also as Fused Deposition Modelling (FDM) technology. Direction of printing was towards one of the long (10 mm) sides. Ultem 1010

material was used, which is amorphous thermoplastic polyetherimide, offering elevated thermal resistance, high strength and stiffness together with broad chemical resistance. Properties of Ultem 1010 material are gathered in Table 4 (Ultem 1010 TDS).

Table 4 - Properties of Ultem 1010

Mechanical properties		
	XZ axis	ZX axis
Yield tensile strength	64 MPa	42 MPa
Tensile modulus	2770 MPa	2200 MPa
Tensile elongation at break	3.3 %	2.0 %
Flexural strength	144 MPa	77 MPa
Flexural modulus	2820 MPa	2230 MPa
Flexural strain at break	No break	3.5 %
Yield compressive strength	134 MPa	107 MPa
Compressive modulus	10000 MPa	1120 MPa
Thermal properties		
Heat deflection temperature @ 66 psi	216 °C	
Heat deflection temperature @ 264 psi	213 °C	
Vicat softening temperature	214 °C	
Glass transition temperature	215 °C	
Coefficient of thermal expansion	47 µm/(m·°C)	
Electrical properties		
Volume resistivity	1.0 x1014 - 8.96x1015 ohm-cm	
Dissipation factor	0.001	
Dielectric strength	240 V/mil	
Other properties		
Density	1270 kg/m3	

The tests were carried out according to (EN ISO 604:2003 standard) using material testing machine as shown in Fig. 13. The test specimen was compressed at constant speed until the specimen fractured or until the load or the decrease in length reached a predetermined value. The load sustained by the specimen was measured during this procedure.

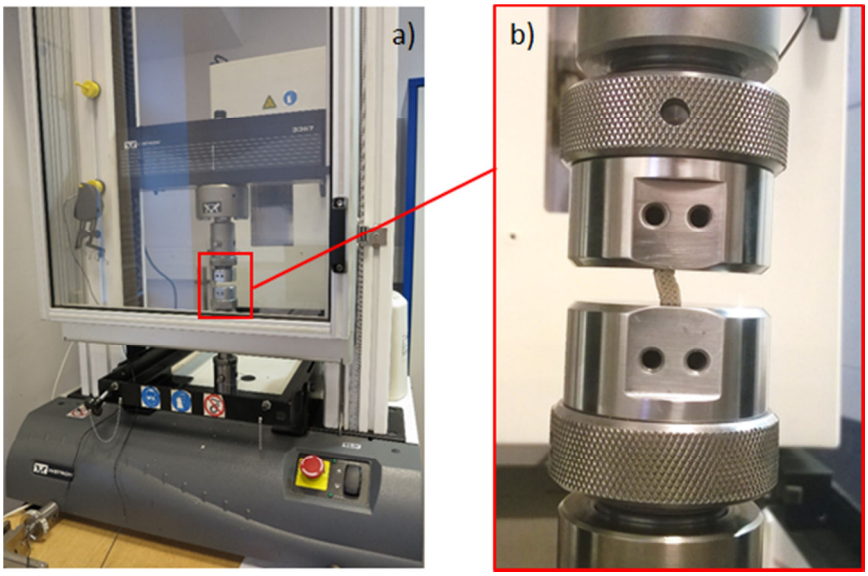

Fig. 13 - Experimental stand for mechanical testing: a) testing machine, b) the tested sample during compression measurement

Fig. 14 illustrates the state of samples after compression tests. It can be seen that honeycomb and lattice structures were broken during the test and split into small pieces, while solid samples were contorted, but remained in one piece. These observations are in line with the values of the measured compressive load depicted in Fig. 15. The highest force on the level of 5087 N acting on the sample was recorded for the solid structure, while for lattice and honeycomb geometry it was on the level of 2582 N and 2355 N respectively.

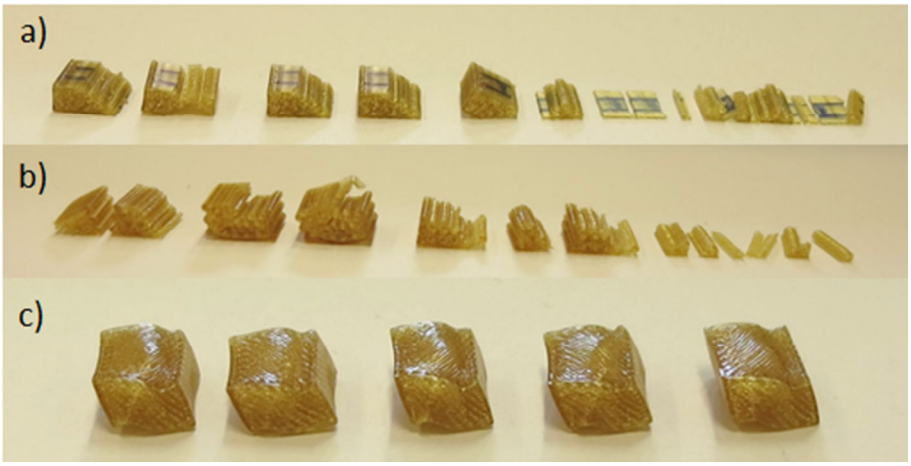

Fig. 14 - Specimens after compression tests: a) honeycomb, b) lattice, c) solid

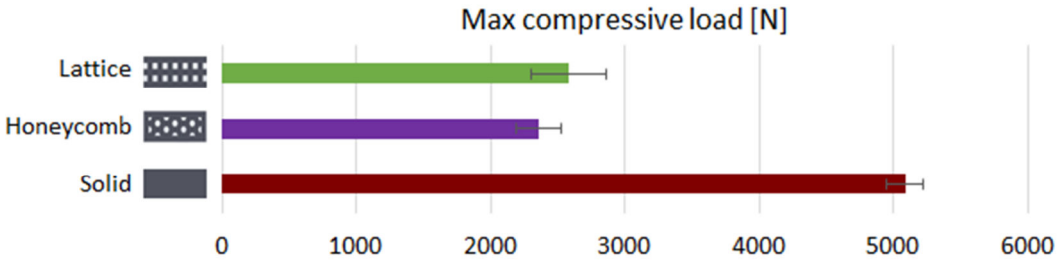

Fig. 15 - Results of compression strength measurements

ELECTRICAL TESTING

In the second step dielectric properties of 3D printed specimens were evaluated. Electrical tests were done on 100x100x4 mm samples 3D printed in FDM process out of Ultem 1010 material. 5 different internal structures of specimens were investigated in electrical tests and for each 6 specimens were tested. Four of them were layered samples and the reference constituted sample having solid structure. The samples are presented in Fig. 15 and the layered structure is additionally described in Table 5.

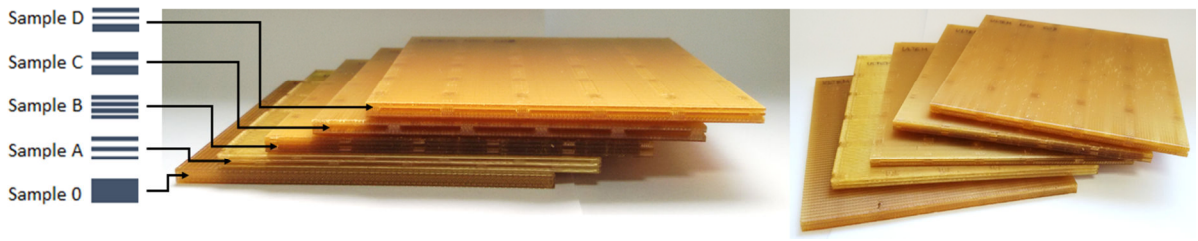

Fig. 15 - Geometries of specimens tested electrically

Table 5 - Layered structures of the tested specimens

No.	Layer	Sample 0	Sample A	Sample B	Sample C	Sample D
1	**plastic**	4 mm	0.8 mm	0.8 mm	1.6 mm	1.6 mm
2	**oil**	-	0.8 mm	0.267 mm	0.8 mm	0.4 mm
3	**plastic**	-	0.8 mm	0.8 mm	1.6 mm	0.8 mm
4	**oil**	-	0.8 mm	0.267 mm	-	0.4 mm
5	**plastic**	-	0.8 mm	0.8 mm	-	0.8 mm
6	**oil**	-	-	0.267 mm	-	-
7	**plastic**	-	-	0.8 mm	-	-
	Total thickness of plastic layers	4 mm	2.4 mm	3.2 mm	3.2 mm	3.2 mm
	Total thickness of oil layers	0 mm	1.6 mm	0.8 mm	0.8 mm	0.8 mm

All samples were tested according to (IEC 60243-1 standard). All samples were preconditioned for 2 hours before measurement in insulating oil having dielectric strength higher than 232 kV/cm. This preconditioning allowed to impregnate samples with insulating oil and to get rid of the problem with air voids that could influence the measurements results.

Experimental stand used in dielectric measurements is shown in Fig. 16. Symmetrical set of circular electrodes having 75 mm of diameter, with rounded edges and made of stainless steel were used. The measured samples were placed between the electrodes and, next, the whole system was immersed in the same insulating oil as the one used for samples preconditioning.

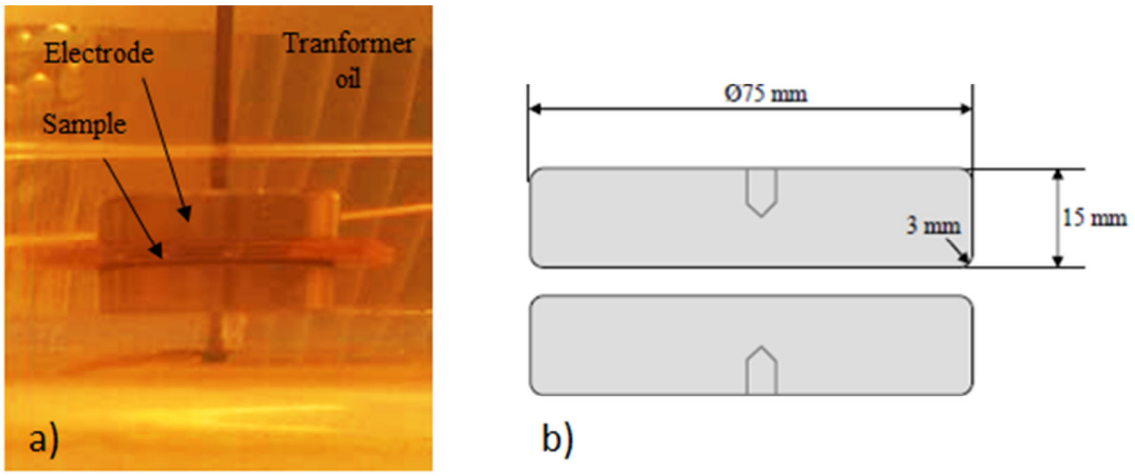

Fig. 16 - Experimental stand used in breakdown voltage measurements: a) sample between electrodes in insulating oil, b) electrode system

Testing procedure applied in breakdown voltage measurements is illustrated in Fig. 17. AC test voltage applied to each sample was increased up to PD inception voltage U_{inc}. Next, PD values were recorded for 15 s, the voltage was decreased to 0 kV and the measurement results were noted. In the subsequent cycle the voltage level was increased above PD inception level by the value being the smallest multiple of number 5 and the measurement was repeated. In the subsequent cycles the test voltage was increased by 5 kV above the value from the previous measurement and results were recorded until sample breakdown at U_{bd} voltage level. If breakdown occurred at the defined voltage level then time between the AC test voltage setting and sample breakdown t_{bd} was also recorded.

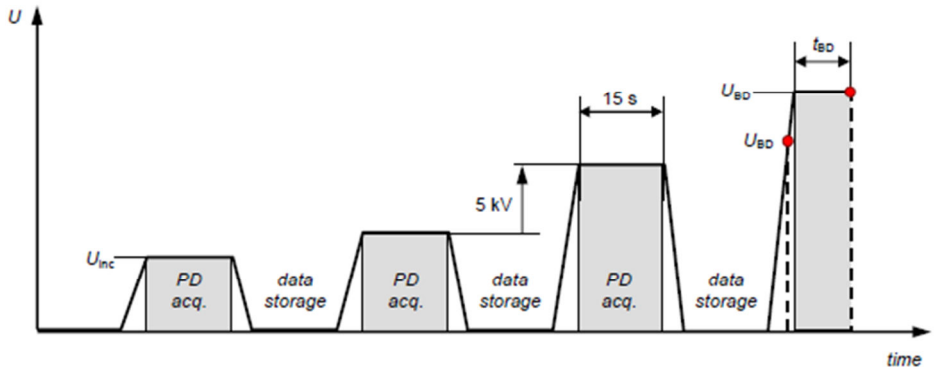

Fig. 17 - Testing procedure applied in breakdown voltage measurements

The results of breakdown voltage measurements are shown in Fig. 18. It is clearly visible that three out of four tested layered samples turned out to be superior when compared to the reference sample having solid structure. From dielectric point of view the weakest geometry was the one consisted of two thick layers of thermoplastic (each having 1.6 mm of thickness) separated by 0.8 mm thick oil layer. Its breakdown voltage was on the level of 22 kV, much below the value observed for the other samples. In turn, the highest voltage before breakdown was withstood by the sample having the highest number of thermoplastic layers (and also the thinnest layers). In this case the average breakdown voltage was equal to 36 kV, a bit higher than for samples A and D. The highest breakdown voltage was measured for one of A type samples and was equal to 41 kV. Additional observation was made when investigating samples after breakdown voltage measurements as presented in Fig. 19. Namely, it can be seen that breakdown occurred in all layered samples in the area of supports connecting the neighbouring layers of thermoplastic material.

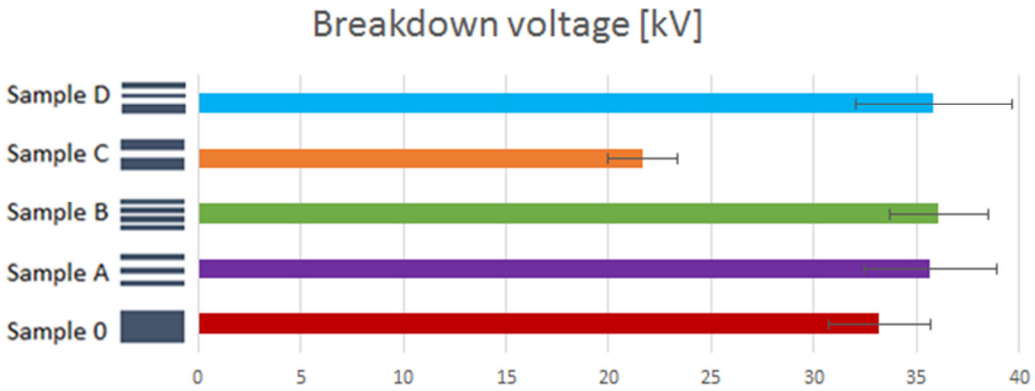

Fig. 18 - Results of breakdown voltage measurements

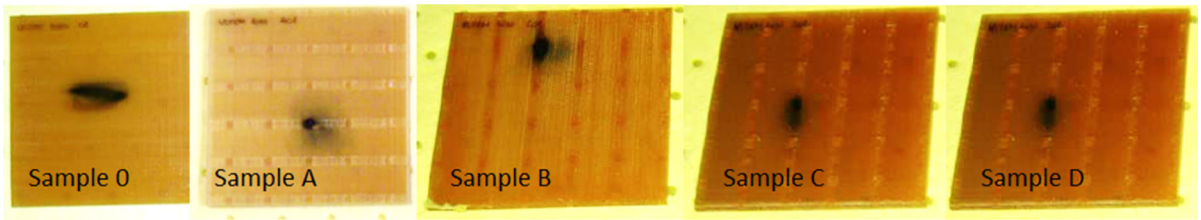

Fig. 19 - Specimens after breakdown voltage measurements

CONCLUSIONS

This study allowed for working out optimum method of composites formulation for 3D printing process resulting in more uniform material composition and less air voids inside the filament. Moreover, the performed numerical simulations and laboratory tests showed that there is a strong influence of geometrical design and printing direction on mechanical parameters. Finally, it was proved that 3D printing technology offering great freedom with respect to geometrical design can be applied as an enabler for improved electrical performance in comparison to the reference parts produced in subtractive manufacturing processes.

REFERENCES

[1]-Zhong W, Li F,Zhang Z, Song L, Li Z. Short fiber reinforced composites for fused deposition modelling. Materials Science and Engineering: A, Vol. 301, Issue 2, 2001, p. 125-130.

[2]-Moulart A, Marrett C, Colton J. Polymeric composites for use in electronic and microwave devices. Polymer Engineering and Science, 2004, Vol. 44, No. 3, p. 588-597.

[3]-Ning F, Cong W, Qiu J, Wei J, Wang S. Additive manufacturing of carbon fiber reinforced thermoplastic composites using fused deposition modelling. Composites Part B, 2015, 80, p. 369-378.

[4]-ABS Filament Material Safety Data Sheet. Shenzhen Esun Industrial Co.

[5]-Carbon Fibre Material Safety Data Sheet. Schwarzwaelder Textil-Werke.

[6]-Ultem 1010 Technical Data Sheet. Stratasys, Ltd.

[7]-EN ISO 604:2003 standard. Plastics - Determination of compressive properties.

[8]-IEC 60243-1 standard. Electrical strength of insulating materials - Test methods - Part 1: Tests at power frequencies.